Disorder Operator and Rényi Entanglement Entropy of Symmetric Mass Generation

Zi Hong Liu,[1] Yuan Da Liao,[2] Gaopei Pan,[2] Menghan Song,[2] Jiarui Zhao,[2] Weilun Jiang,[3] Chao-Ming Jian,[4] Yi-Zhuang You,[5] Fakher F. Assaad,[1,*] Zi Yang Meng,[2,†] and Cenke Xu[6,‡]

[1]*Institut für Theoretische Physik und Astrophysik and Würzburg-Dresden Cluster of Excellence ct.qmat, Universität Würzburg, 97074 Würzburg, Germany*
[2]*Department of Physics and HKU-UCAS Joint Institute of Theoretical and Computational Physics, The University of Hong Kong, Pokfulam Road, Hong Kong SAR, China*
[3]*State Key Laboratory of Quantum Optics and Quantum Optics Devices, Institute of Opto-Electronics, Shanxi University, Taiyuan 030006, China*
[4]*Department of Physics, Cornell University, Ithaca, New York, USA*
[5]*Department of Physics, University of California, San Diego, California 92093, USA*
[6]*Department of Physics, University of California, Santa Barbara, California 93106, USA*

(Received 6 September 2023; revised 22 November 2023; accepted 23 March 2024; published 12 April 2024)

The "symmetric mass generation" (SMG) quantum phase transition discovered in recent years has attracted great interest from both condensed matter and high energy theory communities. Here, interacting Dirac fermions acquire a gap without condensing any fermion bilinear mass term or any concomitant spontaneous symmetry breaking. It is hence beyond the conventional Gross-Neveu-Yukawa-Higgs paradigm. One important question we address in this Letter is whether the SMG transition corresponds to a true unitary conformal field theory. We employ the sharp diagnosis including the scaling of disorder operator and Rényi entanglement entropy in large-scale lattice model quantum Monte Carlo simulations. Our results strongly suggest that the SMG transition is indeed an unconventional quantum phase transition and it should correspond to a true $(2+1)d$ unitary conformal field theory.

DOI: 10.1103/PhysRevLett.132.156503

Introduction and motivation.—When a quantum critical point (continuous quantum phase transition) does not have a Landau-Ginzburg type of description in terms of a local order parameter, it is often referred to as an unconventional quantum critical point (QCP). In this Letter we carefully investigate a class of candidate unconventional QCPs involving Dirac fermions, which were proposed to be beyond the "traditional" paradigm. When we discuss QCPs involving Dirac fermions, the standard paradigm is the Gross-Neveu-Yukawa-Higgs mechanism, in which a bosonic field would couple with the Dirac mass operator, and when the bosonic field condenses, the Dirac fermions acquires a mass [1–4]. The bosonic field carries certain representation of a symmetry group (or gauge group), hence the bosonic field plays the same role as the order parameter in the Landau-Ginzburg theory. In this conventional paradigm, the Dirac fermions acquire a mass through spontaneously breaking certain symmetry. This is essentially the mechanism for the mass generation of all the matter fields in the standard model of particle physics. However, in recent years it was discovered by both condensed matter and high energy physics communities that, under the right conditions, the Dirac fermions can acquire a mass continuously through a QCP *without* breaking any symmetry. This mechanism is called the "symmetric mass generation" (SMG) [5–21]. The possibility of SMG in $(2+1)d$ is tightly related to the classification of interacting topological insulators or topological superconductors in three spatial dimensions, please refer to Ref. [5] for more discussions.

Another archetypal unconventional QCP is the "deconfined quantum critical point" (DQCP) between the Néel and valence bond solid orders, supposedly realized in certain frustrated spin-$1/2$ quantum magnets on the square lattice [22,23]. In the last two decades, the nature of the DQCP has been studied with enormous efforts analytically, numerically, and experimentally [1,2,22–68]. Great progress has been made regarding its potential emergent SO(5) symmetries [27,37,38,47], the surrounding duality web [40,41], and the connection to the symmetry protected topological phase in the higher dimension [69], etc. However, despite all of this progress, the very nature of the DQCP, i.e., whether it corresponds to a true $(2+1)d$ unitary conformal field theory (CFT) or not, remains controversial. One indication that the DQCP should not be a true CFT is that, it "failed" a series of general standards that all $(2+1)d$ unitary CFTs are expected to meet. These standards include the universal logarithmic contribution to both the disorder operator and the entanglement entropy defined in a subregion of the $2d$ space, when the subregion involves sharp corners [55,59,70–73].

Compared with the DQCP, the nature of SMG is even more difficult to address employing analytical techniques such as field theory due to the lack of a controlled limit (for example, a generalization to a controlled large-N limit), though a candidate field theory has been proposed in Refs. [13,14]. Hence, we need to resort to numerical techniques. The previous quantum Monte Carlo (QMC) simulations suggest that the SMG could indeed be a continuous phase transition, i.e., the QCP of SMG indeed appears to be a $(2+1)d$ CFT [5–8,10], as the computed Dirac fermion mass increases continuously from zero at a critical strength of interaction. But the nature of SMG still needs to be tested using the same standards as DQCP on general grounds. In this Letter, we will employ the "tests" that the DQCP failed to pass: the scaling of disorder operator and the Rényi entanglement entropy from lattice model QMC simulations.

Models and numerical settings.—We study the following Hamiltonian on the honeycomb lattice

$$\hat{H} = -t\sum_{\langle ij\rangle,\alpha}(-1)^{\alpha}(\hat{c}^{\dagger}_{i\alpha}\hat{c}_{j\alpha} + \hat{c}^{\dagger}_{j\alpha}\hat{c}_{i\alpha}) + V\sum_{i}(\hat{c}^{\dagger}_{i1}\hat{c}_{i2}\hat{c}^{\dagger}_{i3}\hat{c}_{i4} + \hat{c}^{\dagger}_{i4}\hat{c}_{i3}\hat{c}^{\dagger}_{i2}\hat{c}_{i1}) \tag{1}$$

where the index $\alpha = 1, 2, 3, 4$ and $\langle\cdots\rangle$ reflect the fermion nearest neighbor hopping. At small V, the low energy physics of this model is captured by eight weakly interacting two-component Dirac fermions. The Hamiltonian Eq. (1) has a global SU(4) symmetry at half-filling, which manifests after a particle-hole transformation of flavors $\alpha = 2, 4$. This model Eq. (1) has been studied with fermion QMC in Ref. [10], where a SMG QCP was found in the ground state of the model while tuning V. Since the phase transition is not driven by spontaneous symmetry breaking, we locate the position of the QCP by the opening of the fermion single particle gap Δ_{sp}, as schematically presented at Fig. 1(a). As shown in Fig. 1(b) and in Supplemental Material (SM) [74] as well as in Ref. [10], the single particle gap after extrapolation to the thermodynamic limit opens at the QCP, $V_c = 2.00(5)$. Reference [10] further showed that at $V > V_c$, there is no apparent symmetry breaking of the SU(4) symmetry in the ground state, and the phase diagram is described by a single phase transition from Dirac semimetal (DSM) at $V < V_c$ to a featureless Mott insulator (FMI) at $V > V_c$. In this Letter, we employ the projector fermion auxiliary field QMC simulations [81–83] with linear system size $L = 3, 6, 9, 12, 15, 18$ and the number of sites $N = 2L^2$ for honeycomb lattice (with four flavors of fermions per site), with projection length scaling as $\Theta = 2L$ to investigate the ground state properties of the system. We also note that similar SMG transitions between DSM and FMI have been observed in interacting staggered fermion on a cubical space-time lattice with global SU(4) symmetry and there is no spontaneous symmetry breaking, i.e., condensation of fermion bilinear, observed from large-scale QMC simulations [6,8].

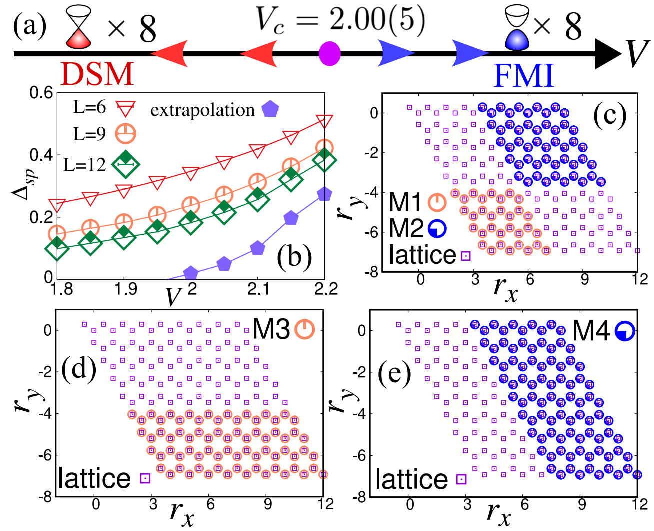

FIG. 1. Phase diagram and entanglement regions. (a) Ground state phase diagram sketch of our lattice model, featuring the SMG QCP at V_c separating the Dirac semimetal (DSM) and featureless Mott insulator (FMI) phases. (b) Fermion single particle gap Δ_{sp} against interaction strength V_c, with the purple curve indicating extrapolated values (refer to SM [74]). (c)–(e) Entanglement regions $M1$, $M2$, $M3$, and $M4$ are highlighted, with $M1$ and $M2$ [orange and blue dots in (c)] utilized for determining corner contributions on the disorder operator. Regions $M3$ [orange dots in (d)] and $M4$ [blue dots in (e)] represent rectangle stripes wrapped around the x and y directions, free from corner contributions.

Numerical probes.—To probe the intrinsic properties of the SMG QCP, we analyze two quantities in QMC simulation. The first one is the disorder operator defined by the symmetry properties of a system [84–87]. For a $(2+1)d$ theory with at least a U(1) symmetry, one can define a disorder operator as

$$\hat{X}_M(\theta) = \prod_{i\in M}\exp(\mathrm{i}\theta\hat{n}_i), \tag{2}$$

where $\hat{n}_i$ is the charge density of the U(1) symmetry at site i. We are interested in the scaling behavior of the disorder operator. If the IR limit of the theory is a $(2+1)d$ CFT, the scaling form of the disorder operator should be dominated by a perimeter law, followed by an additive logarithmic corrections when the region M has corners [88–90],

$$\ln|X_M(\theta)| \sim -al + s(\theta)\ln\, l + c, \tag{3}$$

where $X_M(\theta) = \langle\hat{X}_M(\theta)\rangle$. In the SM, we present a proof that $s(\theta)$ must be non-negative for all θ, for a class of unitary theories [74].

It has been shown that the disorder operator can be conveniently computed in many numerical methods such as QMC and density-matrix renormalization group. The scaling properties of the disorder operator for $(2+1)d$ transverse field Ising, O(2), O(3), topological ordered state and Gross-Neveu transitions have been successfully carried out [71,72,89,91–93], and for these theories the log coefficients of the disorder operators find agreement with unitary CFTs. On the other hand for models that supposedly realize the DQCP (both in spin and fermion realizations) [71,72], the scaling of the disorder operator suggests that the transition is not a unitary CFT.

Since the model Hamiltonian in Eq. (1) has SU(4) flavor symmetry at half-filling [10], we employ the U(1) charge density operator

$$\hat{n}_i = \sum_{\alpha=1}^{4} \hat{n}_{i\alpha} - 2, \tag{4}$$

which is one of the SU(4) symmetry generators. To extract the subleading logarithmic coefficient $s(\theta)$ in a reliable way, we introduce a new partition strategy to cancel the dominant perimeter law contribution. Following Refs. [89,94], we introduce the ratio $P_M(\theta)$

$$P_M(\theta) = \left| \frac{X_{M1}(\theta) X_{M2}(\theta)}{X_{M3}(\theta) X_{M4}(\theta)} \right|, \tag{5}$$

where $M1$ and $M2$ are the two distinct entanglement regions, shown in Fig. 1(c), with the same corner contribution. On the torus geometry, the entanglement regions $M3$ and $M4$ in Figs. 1(d) and 1(e) with shape of $L \times L/2$ are smooth such that the disorder operator is free from corner corrections. Since the length of the boundary of $M1 \cup M2$ is equal to that of $M3 \cup M4$, the leading perimeter law scaling is canceled in the quotient $P_M(\theta)$ and we expect $P_M(\theta) \sim l^{2s(\theta)}$. Extracting $s(\theta)$ from $P_M(\theta)$ turns out to be much more reliable than a direct fit of $X_M(\theta)$ following Eq. (3).

We also calculate the 2nd order Rényi entanglement entropy (EE) $S_M^{(2)}$. A numerically *cheap* QMC calculation of the EE [95,96] for interacting fermions turns out to be unstable such that a replicated space-time manifold [97–99] has to be used. This increases the computational complexity which scales as βN^3 for fermion QMC where $\beta = 1/T$ the inverse temperature and $N = 2L^2$ for one replica of our honeycomb lattice model. The aforementioned numerical instabilities can be cured by an incremental algorithm developed recently [55,100,101]. Here, we further employ the improved protocol developed by one of us [102] to obtain accurate evaluations of the EE.

Results of disorder operator.—Figure 2 shows our results of $\ln|P_M(\theta)|$ versus $\ln(l)$ for various θ and V values. According to Eq. (5), the slope of the curves give rise to the log coefficient $s(\theta)$ and the obtained results are shown in Fig. 3(a). As was pointed out in previous works [72,88,89,103], for small θ, the log-coefficient $s(\theta)$ arising from the corner of the subsystem is proportional to the charge conductivity σ, which is a universal quantity associated with a $(2+1)d$ CFT [104]. More precisely, $s(\theta) \sim \alpha_s \theta^2$ for small θ, and the coefficient α_s is proportional to σ. For example, for a single two-component Dirac fermion in $(2+1)d$ in a region with a sharp corner φ, it will lead to the following result for the coefficient α_s [88,90]:

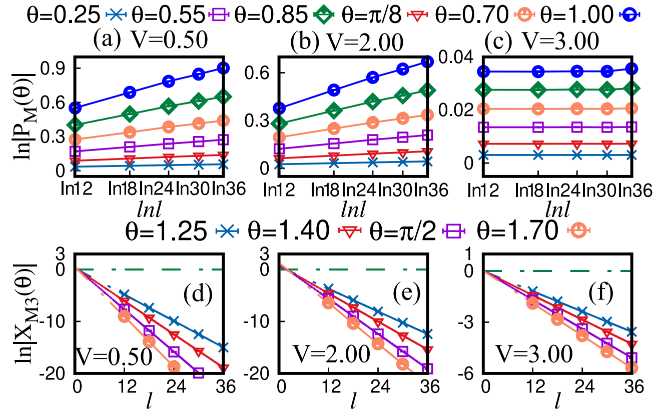

FIG. 2. Disorder operators. Top panels: $\ln|P_M(\theta)|$ [Eq. (5)] as a function of the perimeter $l = 2L$ in the DSM phase (a), at the SMG QCP (b) and in the FMI phase (c). Data suggest $P_M(\theta) \sim l^{2s(\theta)}$. Bottom panels: The disorder operator $\ln|X_{M3}(\theta)|$ as function of perimeter l in the DSM phase (d), at the SMG QCP (e) and in the FMI phase (f). In the absence of corners, $\ln|X_{M3}(\theta)| \sim -al + \beta(\theta)$.

$$\alpha_s = \frac{1}{32\pi^2}[1 + (\pi - \varphi)\cot\varphi]. \tag{6}$$

Both subregions M_1 and M_2 have two angles with $\varphi = 2\pi/3$, and $\pi/3$, and, in our case, we have $N_f = 8$ flavors of Dirac fermion. Thus, for $V < V_c$, in the DSM phase, the theoretical prediction is $\alpha_s \sim 0.132$, independent of V. In Fig. 3(c), the numerical value of α_s within the DSM phase stays roughly constant and is larger than the theoretical value indicated by the green dot. The deviation between the numerical results and analytical value and the weak V dependence on α_s inside DSM phase are due to the finite correlation length in QMC simulations. In SM [74], we provide a mean field analysis to illustrate the finite size effect on computing α_s. We show the value of α_s monotonically converge to the value in the thermodynamic limit by increasing the correlation length at $V = 0$.

The SMG transition is essentially a semimetal-insulator transition, intuitively we expect the conductivity at the SMG to be smaller than that in the Dirac semimetal phase. Indeed, the ratio $\alpha_s(V = V_c)/\alpha_s(V = 0)$ is smaller than 1 in our simulation [shown in the inset of Fig. 3(c)]. It is also the case for the previously investigated Gross-Neveu transition of Dirac fermions, which is also a semimetal-insulator transition [72,93]. But we would like to remark

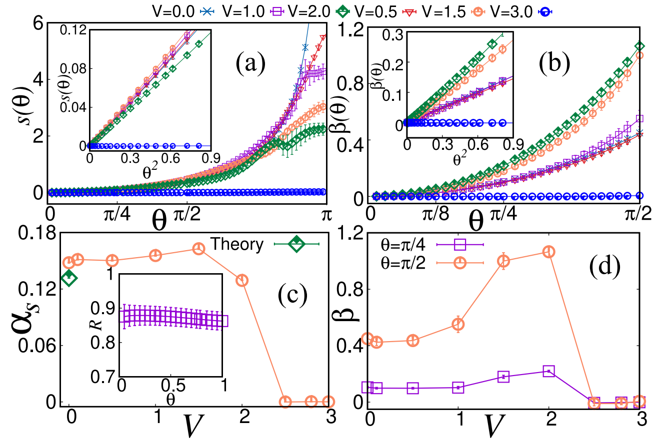

FIG. 3. Logarithmic correction $s(\theta)$ of the disorder operator. (a) Logarithmic coefficient $s(\theta)$ extracted from $P_M(\theta)$ in top panels of Fig. 2. $s(\theta)$ is positive for all the rotation angle $\theta \in [0, \pi]$. (b) The constant correction $\beta(\theta)$ extracted from the disorder operator in the bottom panels of Fig. 2, defined in smooth region $M3$ as a function of rotation angle θ. Insets in (a) and (b) show the x axis rescaled to θ^2, reflecting quadratic angle dependence of $s(\theta)$ and $\beta(\theta)$. (c) The quadratic coefficient α_s of $s(\theta) \sim \alpha_s \theta^2$ reduces at the SMG QCP and vanish in the FMI phase. Inset in (c) presents the ratio $R = \{[s(\theta, V = V_c)]/[s(\theta, V = 0)]\} < 1$ at small θ, analogous to the Gross-Neveu transition discussed in Ref. [72]. (d) $\beta(\theta)$ from (b) with two specific θ values ($\pi/4$ and $\pi/2$) as a function of V, a peak of β develops at V_c and then drops to zero at $V > V_c$.

that, unlike the EE, there is no general theorem which directly connects the RG flow with the magnitude of σ.

It was shown numerically that, at the DQCP $s(\theta)$ can become negative for a broad range of θ [71,72], if one tries fitting the data of the disorder operator with the form of Eq. (3), which is in stark contrast against the general conclusion of the non-negativity of $s(\theta)$ for all θ. In our model, as shown in Fig. 3(a), $s(\theta)$ indeed remains positive for all θ and $V \le V_c$, which is analogous to the situation of the Gross-Neveu transition. When $V > V_c$, $s(\theta) = 0$ since the system is gapped and featureless.

If the subregion M has a smooth boundary, i.e., there is no corner, we expect that the disorder operator scales as $\ln|X_M(\theta)| \sim -al + \beta(\theta)$, with a constant $\beta(\theta)$ which also encodes the information of the CFT. The reason for this expectation is that the conserved charge density that was used to construct the disorder operator is dual to the Wilson loop operator, using the standard dictionary of duality in $(2+1)d$, and the Wilson loop operator can be viewed as a $1d$ defect inserted in the $(2+1)d$ CFT. A quantity similar to $\beta(\theta)$ defined in flat spacetime is referred to as "defect entropy" in Ref. [105]. In Fig. 3(b) we show $\beta(\theta)$ and the inset exhibits $\beta(\theta)$ versus θ^2. Taking two specific θ values of $\pi/4$ and $\pi/2$, we observe that $\beta(\theta)$ is finite for $V \le V_c$, develops a peak close to V_c and a vanishes in the FMI phase, as shown in Fig. 3(d).

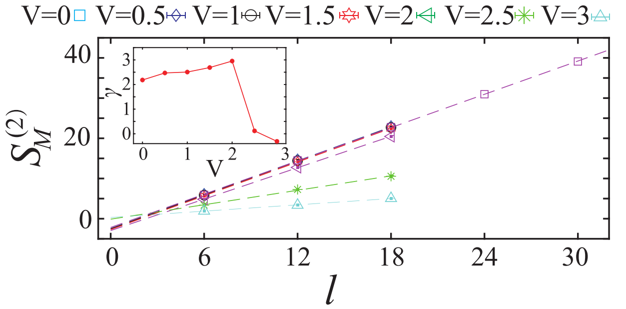

FIG. 4. Entanglement entropy. Finite size scaling relation $S_M^{(2)} = al - \gamma$ of the EE for the bipartition with subregion $L \times L/3$ and $l = 2L$. The intercept term γ crucially characterizes scaling behavior for different phases. At the SMG QCP $V = V_c$, $\gamma(V_c)$ peaks compared to $\gamma(V < V_c)$ governed by the free Dirac CFT. Entering the FMI phase at $V > V_c$, $\gamma(V > V_c)$ approaches zero, akin to $s(\theta)$ and $\beta(\theta)$ in Fig. 3.

Results of entanglement entropy.—Figure 4 shows our results for the EE for various V values, for corner-free bipartitions of size $L \times L/3$ for $L = 3$, 6, 9 as shown in Figs. 1(d) and 1(e). Since there is no corner contribution in our measurement, we expect the EE to exhibit the scaling form of $S_M^{(2)} = al - \gamma$ with $l = 2L$. As shown in Ref. [106], the constant term γ of the EE on a torus depends on several global geometric parameters of the entire system and the subregion. In Fig. 4, we see that the EE is dominated by the perimeter law for all values of V. In the inset, we plot the intercepts γ as a function of V and observe a maximum at $V = V_c$. Interestingly, we find that $\beta(\theta)$ from the disorder operator with smooth boundary and $\theta = \pi/2$ behaves similarly to γ from EE, where $S_M^{(2)}$ and X_M map onto each other for noninteracting problems [93].

Discussions.—In summary, we investigated three quantities that should encode important universal information of the IR behavior of the SMG transition: (1) For a subregion M with sharp corners, the disorder operator $\hat{X}_M(\theta)$ should scale as $\ln|X_M(\theta)| \sim -al + s(\theta) \ln l$, where $s(\theta)$ is a universal quantity related to the universal conductivity of the $(2+1)d$ CFT [90,107–109]; and $s(\theta)$ should be non-negative for all θ, for a large class of unitary $(2+1)d$ CFT (see SM [74]). (2) For a smooth subregion M without corner, the disorder operator $\hat{X}_M(\theta)$ scales as $\ln|X_M(\theta)| \sim -al + \beta(\theta)$, and $\beta(\theta)$ peaks at the SMG QCP. (3) For a smooth subregion M without corner, the second Rényi EE scales as $S_M^{(2)} \sim al - \gamma$, where γ is also a universal quantity, which peaks at the SMG QCP.

The three universal quantities, i.e., $s(\theta)$, $\beta(\theta)$, and γ are all nonzero in the Dirac semimetal phase as well as the SMG QCP, and all vanish inside the FMI phase. In particular, $s(\theta)$ remains positive for all θ at the SMG QCP. These findings strongly suggest that the SMG transition indeed corresponds to a true $(2+1)d$ unitary

CFT, without violating the non-negativity bound as in the case of DQCP.

Various mysteries regarding the SMG transition still remain. For instance, the Dirac semimetal phase with $V < V_c$ should have a large emergent SO(16) symmetry, which manifests when one Dirac fermion is expressed as two Majorana fermions. Although the lattice model breaks SO(16) symmetry, it is the maximal possible emergent symmetries of the IR fixed points. Whether this SO(16) symmetry (or its subgroup) can emerge at the SMG transition remains uncertain. Future investigations should examine the disorder operator associated with the generators of SO(16) to ascertain the full emergent symmetry at the SMG. Additionally, verifying the universal corner-log correction of EE at the SMG QCP is pertinent. Because of computational constraints in our current model, extracting this information was unfeasible. However, we aim to explore it using more efficient algorithms in the future.

The authors thank Yin-Chen He and Meng Cheng for very helpful discussions. Z. H. L. acknowledges the Deutsche Forschungsgemeinschaft through the Würzburg-Dresden Cluster of Excellence on Complexity and Topology in Quantum Matter–*ct.qmat* (EXC 2147, Project No. 390858490). G. P. P., M. H. S., J. R. Z., W. L. J., and Z. Y. M. acknowledge the support from the Research Grants Council of Hong Kong Special Administrative Region (SAR) of China (Projects No. 17301721, No. AoE/P701/20, No. 17309822, No. C7037-22GF, and No. 17302223), the ANR/RGC Joint Research Scheme sponsored by the RGC of Hong Kong SAR of China and French National Research Agency (Project No. A_HKU703/22), and the Beijng PARATERA Tech CO., Ltd. [110] for providing HPC resources that have contributed to the research results reported within this Letter. Y. D. L. acknowledges support from National Natural Science Foundation of China (Grant No. 12247114). Y. Z. Y. is supported by the National Science Foundation (Grant No. DMR-2238360). C. X. is supported by the Simons Investigator program. C.-M. J. is supported by a faculty startup grant at Cornell University. F. F. A. acknowledges financial support from the German Research Foundation (DFG) under the Grant No. AS 120/16-1 (Project No. 493886309) that is part of the collaborative research project SFB Q-M&S funded by the Austrian Science Fund (FWF) F 86. F. F. A. and Z. H. L. gratefully acknowledge the Gauss Centre for Supercomputing e.V. [111] for funding this project by providing computing time on the GCS Supercomputer SUPERMUC-NG at Leibniz Supercomputing Centre [112] (Project No. pn73xu), as well as the scientific support and HPC resources provided by the Erlangen National High Performance Computing Center (NHR@FAU) of the Friedrich-Alexander-Universität Erlangen-Nürnberg (FAU) under the NHR Project No. b133ae. NHR funding is provided by federal and Bavarian state authorities. NHR@FAU hardware is partially funded by the German Research Foundation (DFG)–440719683. The calculations for the disorder operator were carried out with the ALF package [113].

*fakher.assaad@physik.uni-wuerzburg.de
†zymeng@hku.hk
‡xucenke@ucsb.edu

[1] Y. D. Liao, X. Y. Xu, Z. Y. Meng, and Y. Qi, Phys. Rev. B **106**, 075111 (2022).
[2] Z. H. Liu, M. Vojta, F. F. Assaad, and L. Janssen, Phys. Rev. Lett. **128**, 087201 (2022).
[3] T. C. Lang and A. M. Läuchli, Phys. Rev. Lett. **123**, 137602 (2019).
[4] Y. Liu, Z. Wang, T. Sato, W. Guo, and F. F. Assaad, Phys. Rev. B **104**, 035107 (2021).
[5] K. Slagle, Y.-Z. You, and C. Xu, Phys. Rev. B **91**, 115121 (2015).
[6] V. Ayyar and S. Chandrasekharan, Phys. Rev. D **91**, 065035 (2015).
[7] S. Catterall, J. High Energy Phys. 01 (2016) 121.
[8] V. Ayyar and S. Chandrasekharan, Phys. Rev. D **93**, 081701(R) (2016).
[9] S. Catterall and D. Schaich, Phys. Rev. D **96**, 034506 (2017).
[10] Y.-Y. He, H.-Q. Wu, Y.-Z. You, C. Xu, Z. Y. Meng, and Z.-Y. Lu, Phys. Rev. B **94**, 241111(R) (2016).
[11] Y. Kikukawa, Prog. Theor. Exp. Phys. **2019**, 073B02 (2019).
[12] Y. Kikukawa, Prog. Theor. Exp. Phys. **2019**, 113B03 (2019).
[13] Y.-Z. You, Y.-C. He, C. Xu, and A. Vishwanath, Phys. Rev. X **8**, 011026 (2018).
[14] Y.-Z. You, Y.-C. He, A. Vishwanath, and C. Xu, Phys. Rev. B **97**, 125112 (2018).
[15] Y. Xu and C. Xu, arXiv:2103.15865.
[16] D. Tong, J. High Energy Phys. 07 (2022) 001.
[17] M. Zeng, Z. Zhu, J. Wang, and Y.-Z. You, Phys. Rev. Lett. **128**, 185301 (2022).
[18] J. Wang and X.-G. Wen, Phys. Rev. B **107**, 014311 (2023).
[19] W. Hou and Y.-Z. You, arXiv:2212.13364.
[20] D.-C. Lu, M. Zeng, J. Wang, and Y.-Z. You, Phys. Rev. B **107**, 195133 (2023).
[21] J. Wang and Y.-Z. You, Symmetry **14**, 1475 (2022).
[22] T. Senthil, A. Vishwanath, L. Balents, S. Sachdev, and M. P. Fisher, Science **303**, 1490 (2004).
[23] T. Senthil, L. Balents, S. Sachdev, A. Vishwanath, and M. P. A. Fisher, Phys. Rev. B **70**, 144407 (2004).
[24] T. Senthil, arXiv:2306.12638.
[25] M. Levin and T. Senthil, Phys. Rev. B **70**, 220403(R) (2004).
[26] T. Senthil, L. Balents, S. Sachdev, A. Vishwanath, and M. P. A. Fisher, J. Phys. Soc. Jpn. **74**, 1 (2005).
[27] T. Senthil and M. P. A. Fisher, Phys. Rev. B **74**, 064405 (2006).
[28] A. W. Sandvik, Phys. Rev. Lett. **98**, 227202 (2007).

[29] R. G. Melko and R. K. Kaul, Phys. Rev. Lett. **100**, 017203 (2008).
[30] J. Lou, A. W. Sandvik, and N. Kawashima, Phys. Rev. B **80**, 180414(R) (2009).
[31] A. Banerjee, K. Damle, and F. Alet, Phys. Rev. B **82**, 155139 (2010).
[32] A. W. Sandvik, Phys. Rev. Lett. **104**, 177201 (2010).
[33] C. Xu, Int. J. Mod. Phys. B **26**, 1230007 (2012).
[34] S. Pujari, K. Damle, and F. Alet, Phys. Rev. Lett. **111**, 087203 (2013).
[35] M. S. Block, R. G. Melko, and R. K. Kaul, Phys. Rev. Lett. **111**, 137202 (2013).
[36] K. Harada, T. Suzuki, T. Okubo, H. Matsuo, J. Lou, H. Watanabe, S. Todo, and N. Kawashima, Phys. Rev. B **88**, 220408(R) (2013).
[37] A. Nahum, J. T. Chalker, P. Serna, M. Ortuño, and A. M. Somoza, Phys. Rev. X **5**, 041048 (2015).
[38] A. Nahum, P. Serna, J. T. Chalker, M. Ortuño, and A. M. Somoza, Phys. Rev. Lett. **115**, 267203 (2015).
[39] H. Shao, W. Guo, and A. W. Sandvik, Science **352**, 213 (2016).
[40] C. Wang, A. Nahum, M. A. Metlitski, C. Xu, and T. Senthil, Phys. Rev. X **7**, 031051 (2017).
[41] Y. Q. Qin, Y.-Y. He, Y.-Z. You, Z.-Y. Lu, A. Sen, A. W. Sandvik, C. Xu, and Z. Y. Meng, Phys. Rev. X **7**, 031052 (2017).
[42] J. D'Emidio and R. K. Kaul, Phys. Rev. Lett. **118**, 187202 (2017).
[43] X.-F. Zhang, Y.-C. He, S. Eggert, R. Moessner, and F. Pollmann, Phys. Rev. Lett. **120**, 115702 (2018).
[44] N. Ma, G.-Y. Sun, Y.-Z. You, C. Xu, A. Vishwanath, A. W. Sandvik, and Z. Y. Meng, Phys. Rev. B **98**, 174421 (2018).
[45] R.-Z. Huang, D.-C. Lu, Y.-Z. You, Z. Y. Meng, and T. Xiang, Phys. Rev. B **100**, 125137 (2019).
[46] B. Roberts, S. Jiang, and O. I. Motrunich, Phys. Rev. B **99**, 165143 (2019).
[47] N. Ma, Y.-Z. You, and Z. Y. Meng, Phys. Rev. Lett. **122**, 175701 (2019).
[48] X. Y. Xu, Y. Qi, L. Zhang, F. F. Assaad, C. Xu, and Z. Y. Meng, Phys. Rev. X **9**, 021022 (2019).
[49] Z.-X. Li, S.-K. Jian, and H. Yao, arXiv:1904.10975.
[50] A. Nahum, Phys. Rev. B **102**, 201116(R) (2020).
[51] R. Ma and C. Wang, Phys. Rev. B **102**, 020407(R) (2020).
[52] G. J. Sreejith, S. Powell, and A. Nahum, Phys. Rev. Lett. **122**, 080601 (2019).
[53] B. Zhao, J. Takahashi, and A. W. Sandvik, Phys. Rev. Lett. **125**, 257204 (2020).
[54] A. W. Sandvik and B. Zhao, Chin. Phys. Lett. **37**, 057502 (2020).
[55] Y. D. Liao, G. Pan, W. Jiang, Y. Qi, and Z. Y. Meng, arXiv:2302.11742.
[56] Z. Zhou, L. Hu, W. Zhu, and Y.-C. He, arXiv:2306.16435.
[57] N. Xi, H. Chen, Z. Y. Xie, and R. Yu, Phys. Rev. B **107**, L220408 (2023).
[58] B.-B. Chen, X. Zhang, Y. Wang, K. Sun, and Z. Y. Meng, arXiv:2307.05307.
[59] M. Song, J. Zhao, L. Janssen, M. M. Scherer, and Z. Y. Meng, arXiv:2307.02547.
[60] M. E. Zayed *et al.*, Nat. Phys. **13**, 962 (2017).
[61] J. Guo, G. Sun, B. Zhao, L. Wang, W. Hong, V. A. Sidorov, N. Ma, Q. Wu, S. Li, Z. Y. Meng, A. W. Sandvik, and L. Sun, Phys. Rev. Lett. **124**, 206602 (2020).
[62] G. Sun, N. Ma, B. Zhao, A. W. Sandvik, and Z. Y. Meng, Chin. Phys. B **30**, 067505 (2021).
[63] Y. Cui, L. Liu, H. Lin, K.-H. Wu, W. Hong, X. Liu, C. Li, Z. Hu, N. Xi, S. Li, R. Yu, A. W. Sandvik, and W. Yu, Science **380**, 1179 (2023).
[64] T. Song, Y. Jia, G. Yu, Y. Tang, P. Wang, R. Singha, X. Gui, A. J. Uzan, M. Onyszczak, K. Watanabe, T. Taniguchi, R. J. Cava, L. M. Schoop, N. P. Ong, and S. Wu, Nat. Phys. **20**, 269 (2024).
[65] Y. Liu, Z. Wang, T. Sato, M. Hohenadler, C. Wang, W. Guo, and F. F. Assaad, Nat. Commun. **10**, 2658 (2019).
[66] Z. Wang, M. P. Zaletel, R. S. K. Mong, and F. F. Assaad, Phys. Rev. Lett. **126**, 045701 (2021).
[67] T. Sato, Z. Wang, Y. Liu, D. Hou, M. Hohenadler, W. Guo, and F. F. Assaad, arXiv:2212.11395.
[68] J. Guo, P. Wang, C. Huang, B.-B. Chen, W. Hong, S. Cai, J. Zhao, J. Han, X. Chen, Y. Zhou, S. Li, Q. Wu, Z. Y. Meng, and L. Sun, arXiv:2310.20128.
[69] A. Vishwanath and T. Senthil, Phys. Rev. X **3**, 011016 (2013).
[70] J. Zhao, Y.-C. Wang, Z. Yan, M. Cheng, and Z. Y. Meng, Phys. Rev. Lett. **128**, 010601 (2022).
[71] Y.-C. Wang, N. Ma, M. Cheng, and Z. Y. Meng, SciPost Phys. **13**, 123 (2022).
[72] Z. H. Liu, W. Jiang, B.-B. Chen, J. Rong, M. Cheng, K. Sun, Z. Y. Meng, and F. F. Assaad, Phys. Rev. Lett. **130**, 266501 (2023).
[73] A summary of these results and more analysis will be presented in an upcoming work.
[74] See Supplemental Material at http://link.aps.org/supplemental/10.1103/PhysRevLett.132.156503, which includes Refs. [75–80], for the proof of positivity of $s(\theta)$ for a class of theories, benchmarking of the entanglement entropy, and disorder operator calculation with the free Dirac fermion systems and the quantum Monte Carlo measurements of Green's function of the SMG Hamiltonian and its phase transition.
[75] H. Casini and M. Huerta, J. High Energy Phys. 11 (2012) 087.
[76] N. Seiberg, T. Senthil, C. Wang, and E. Witten, Ann. Phys. (Amsterdam) **374**, 395 (2016).
[77] E. Fradkin and J. E. Moore, Phys. Rev. Lett. **97**, 050404 (2006).
[78] I. Peschel, J. Phys. A **36**, L205 (2003).
[79] H. Casini and M. Huerta, J. Phys. A **42**, 504007 (2009).
[80] J. Helmes, L. E. Hayward Sierens, A. Chandran, W. Witczak-Krempa, and R. G. Melko, Phys. Rev. B **94**, 125142 (2016).
[81] G. Sugiyama and S. Koonin, Ann. Phys. (N.Y.) **168**, 1 (1986).
[82] S. Sorella, S. Baroni, R. Car, and M. Parrinello, Europhys. Lett. **8**, 663 (1989).
[83] F. Assaad and H. Evertz, in *Computational Many-Particle Physics* (Springer, New York, 2008), pp. 277–356.
[84] E. Fradkin, J. Stat. Phys. **167**, 427 (2017).
[85] Z. Nussinov and G. Ortiz, Proc. Natl. Acad. Sci. U.S.A. **106**, 16944 (2009).

[86] Z. Nussinov and G. Ortiz, Ann. Phys. (Amsterdam) **324**, 977 (2009).
[87] L. P. Kadanoff and H. Ceva, Phys. Rev. B **3**, 3918 (1971).
[88] X.-C. Wu, C.-M. Jian, and C. Xu, SciPost Phys. **11**, 033 (2021).
[89] Y.-C. Wang, M. Cheng, and Z. Y. Meng, Phys. Rev. B **104**, L081109 (2021).
[90] B. Estienne, J.-M. Stéphan, and W. Witczak-Krempa, Nat. Commun. **13**, 287 (2022).
[91] J. Zhao, Z. Yan, M. Cheng, and Z. Y. Meng, Phys. Rev. Res. **3**, 033024 (2021).
[92] B.-B. Chen, H.-H. Tu, Z. Y. Meng, and M. Cheng, Phys. Rev. B **106**, 094415 (2022).
[93] W. Jiang, B.-B. Chen, Z. H. Liu, J. Rong, F. F. Assaad, M. Cheng, K. Sun, and Z. Y. Meng, SciPost Phys. **15**, 082 (2023).
[94] A. B. Kallin, E. Stoudenmire, P. Fendley, R. R. Singh, and R. G. Melko, J. Stat. Mech. (2014) P06009.
[95] T. Grover, Phys. Rev. Lett. **111**, 130402 (2013).
[96] F. F. Assaad, T. C. Lang, and F. Parisen Toldin, Phys. Rev. B **89**, 125121 (2014).
[97] P. Calabrese and J. Cardy, J. Stat. Mech. (2004) P06002.
[98] F. F. Assaad, Phys. Rev. B **91**, 125146 (2015).
[99] P. Broecker and S. Trebst, J. Stat. Mech. (2014) P08015.
[100] J. D'Emidio, R. Orus, N. Laflorencie, and F. de Juan, Phys. Rev. Lett. **132**, 076502 (2024).
[101] G. Pan, Y. D. Liao, W. Jiang, J. D'Emidio, Y. Qi, and Z. Y. Meng, Phys. Rev. B **108**, L081123 (2023).
[102] Y. D. Liao, arXiv:2307.10602.
[103] Y.-C. Wang, M. Cheng, W. Witczak-Krempa, and Z. Y. Meng, Nat. Commun. **12**, 5347 (2021).
[104] Here the conductivity σ is in the AC limit, i.e. in the limit $\omega/T \to \infty$, and $T \to 0$.
[105] G. Cuomo, Z. Komargodski, and A. Raviv-Moshe, Phys. Rev. Lett. **128**, 021603 (2022).
[106] X. Chen, W. Witczak-Krempa, T. Faulkner, and E. Fradkin, J. Stat. Mech. (2017) 043104.
[107] S. Giombi, G. Tarnopolsky, and I. R. Klebanov, J. High Energy Phys. 08 (2016) 156.
[108] K. Diab, L. Fei, S. Giombi, I. R. Klebanov, and G. Tarnopolsky, J. Phys. A **49**, 405402 (2016).
[109] Y. Huh, P. Strack, and S. Sachdev, Phys. Rev. B **88**, 155109 (2013).
[110] https://cloud.paratera.com.
[111] http://www.gauss-centre.eu.
[112] http://www.lrz.de.
[113] F. F. Assaad, M. Bercx, F. Goth, A. Götz, J. S. Hofmann, E. Huffman, Z. Liu, F. P. Toldin, J. S. E. Portela, and J. Schwab, SciPost Phys. Codebases 1 (2022) 10.21468/SciPostPhysCodeb.1.